Lipomeningomyelocystocele.

A Vade and D Kennard

AJNR Am J Neuroradiol 1987, 8 (2) 375-377
http://www.ajnr.org/content/8/2/375.citation

Lipomeningomyelocystocele

Aruna Vade[1] and Donald Kennard

Conventional radiography coupled with myelography has long been used in evaluating spinal dysraphism in children [1, 2]. Recently, CT and sonography have also been used [3–6]. To our knowledge, this is the first reported case of lipomeningomyelocystocele evaluated by radiographic, sonographic, and MR imaging techniques. This report compares these three imaging methods in terms of their effectiveness in evaluating a patient with surgically proven lipomeningomyelocystocele.

Case Report

A full-term infant girl who underwent a normal, spontaneous, vaginal delivery was born with multiple congenital anomalies, including an omphalocele, extrophy of bladder, indeterminate genitalia, imperforate anus, hydronephrotic left kidney, and a large swelling over the back. Her karyotype was 46 XX; she was born to a Hispanic, diabetic mother.

Cranial sonography on the second day of birth was normal. Sonographic scanning of the cystic mass over the back was done with real-time and static B-mode scanners. Two fluid-filled sacs were identified (Fig. 1). The inner and more caudal of the two sacs had multiple septations between anechoic spaces, whereas the outer and more cranial sac was completely anechoic. The caudal septated sac was continuous with the spinal canal. No such communication with the spinal canal was evinced by the anechoic outer sac.

CT of the spine revealed a cystlike structure measuring 15–30 H posterior to the spine. A differentiation between a meningocele and meningomyelocele could not be made. Dysraphism of lumbar vertebrae was also noted.

A metrizamide myelogram was then done by injection at the T12 level, just above the cranial limit of the cystic mass on the back. This site was chosen because a prior attempt to inject metrizamide by cervical puncture had failed. The contrast material flowed cranially to the T9 level, and no spinal cord was seen from the T9 to the T12 levels. Posterior to the spine, a cystic cavity filled with contrast material was seen surrounded by a soft-tissue component. The contrast-filled cavity corresponded to the inner caudal sac identified by sonography and MR.

A postmyelogram CT scan of the spine (Fig. 2) and head was also obtained. Metrizamide was seen in the spinal canal cranial to spina bifida cystica with no visualization of the spinal cord. The contrast material in the spinal canal was continuous with the contrast-filled cystic structure posterior to the spine. More posterior to the contrast-filled cystic structure was another, nonopacified, cystic structure with fluid density of 10–15 H. A CT scan of the head did not locate metrizamide in the ventricles. From this study it was presumed that the outer sac was continuous proximally with a hydromyelia that was encircled by a very thin spinal cord. Adipose tissue was seen inferior to the caudal sac on lower sacral spine sections.

MR imaging was done in transverse and sagittal planes with a spin-echo technique of 30-msec echo time and 500-msec repetition time (Fig. 3). Two cystic components of different signal strengths were seen on MR images of the swelling on the back. The inner sac was seen to be continuous with the spinal canal. Fat was seen inferior and adjacent to the caudal and inner cystic component, and was believed to be a lipoma associated with swelling over the back. It was separated from the subcutaneous fat, seen farther down, by a thin septa.

Reconstructive surgery for the cystic mass on the lower back was performed. The outer sac was slit open and its cyst walls excised and sent for histopathologic confirmation, which revealed gliotic neurophils in fibroadipose tissue covered by hyaline cartilage, fibrocartilage, subcutaneous fibroadipose tissue, and skin on one side and ependyma on the other side. The tissues from the outer sac wall were consistent with a myelocele. The outer sac was seen to be continuous with the central canal proximally, thus further confirming the diagnosis of a dilated and herniated central canal. Part of the inner sac, which contained the nerve roots, was excised and, on histopathology, showed cells resembling arachnoid cells lining the wall on one side. The nerve roots were subsequently placed within the spinal canal.

Discussion

There are two theories proposed for the pathogenesis of spina bifida cystica. The least accepted theory attributes it to rupture of a normally formed neural tube caused by increased CSF pressure from hydrocephalus [7, 8]. The most accepted theory holds failure of neuralation responsible [8, 9]. Neuralation means closure of the neural tube by fusion of the edges of the neural groove. This starts in the cervical region, spreads in a cranial and caudal direction, and is complete by 24–26 days gestational age. If the developmental defect occurs before 24 days gestational age, myeloschisis results, in which a flat, neural, platelike structure appears at the surface with no overlying vertebra or dermal covering [7]. Spina bifida cystica occurs as a result of developmental defects acquired between 24–26 days gestational age [7]. Eighty percent of all spina bifida cysticas occur in the lumbar region, which is

Received January 18, 1985; accepted after revision July 9, 1985.
[1] Both authors: Department of Radiology, University of Illinois Hospital, 1740 W. Taylor Street, Chicago, IL 60612. Address reprint requests to A. Vade.

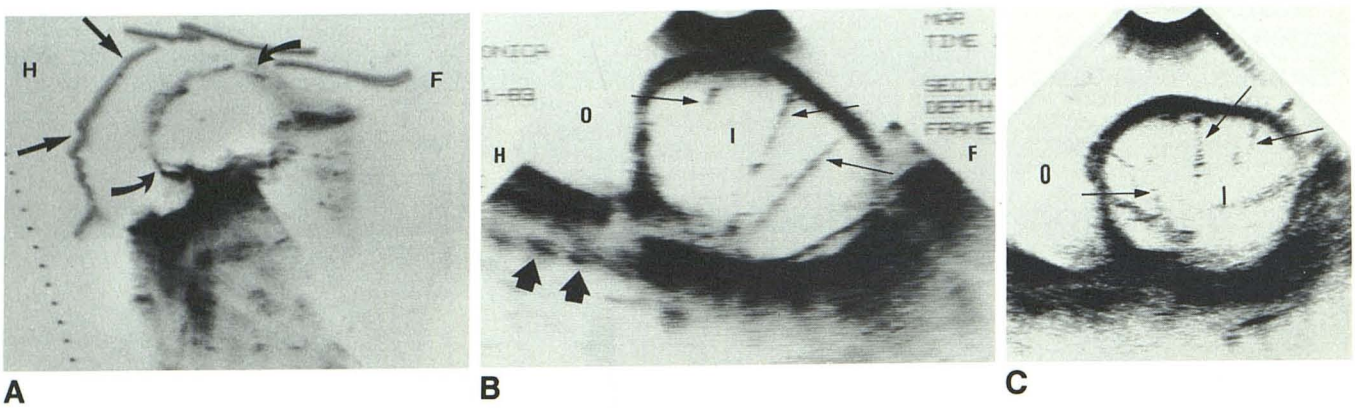

A B C

Fig. 1.—*A*, Midline longitudinal sonogram of cystic mass from T12 to lower sacrum, with static B-mode scanner, shows outer sac (*straight arrows*) and inner sac (*curved arrows*). (H = head end, F = foot end.)

***B*, Longitudinal real-time sonogram over cystic mass obtained to show continuation of inner sac (I) with spinal canal (*thick arrows*). Within inner sac are multiple septations that represent nerve roots (*thin arrows*). Outer sac (O) is incompletely seen on this sector scan. (H = head end, F = foot end.) Note that inner cyst loses its sonolucency as it enters spinal canal because of crowding together of nerve roots.**

***C*, Transverse real-time sonogram over middle portion of cystic mass shows inner sac (I) with multiple septations (*arrows*) that represent nerve roots. Outer sac (O) is partly seen.**

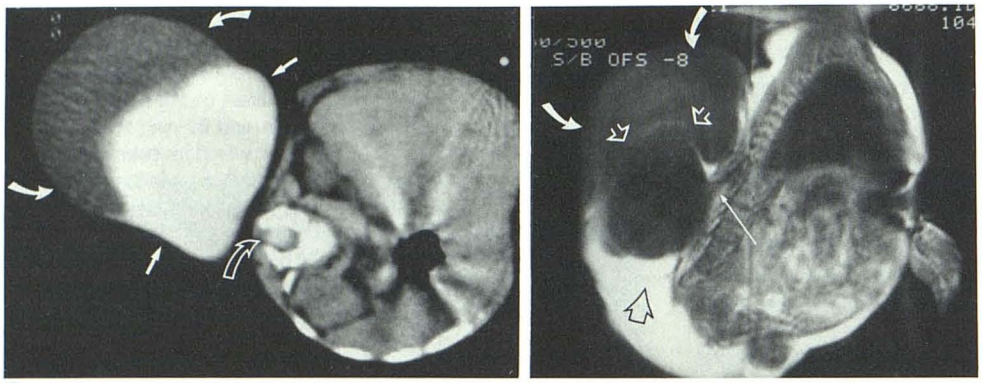

2 3

Fig. 2.—Axial section from metrizamide CT scan of spine at level of second lumbar vertebra shows contrast within inner sac (*straight arrows*) and spinal canal (*open arrow*). Outer sac (*curved solid arrows*) shows fluid density of 10–15 H.

Fig. 3.—MR image of cystic mass in sagittal plane with spin-echo technique (echo time = 30 msec, repetition time = 500 msec) demonstrates the two cystic components showing different signal intensities. Outer sac (*curved arrows*) has higher signal intensity than inner sac (*open arrowheads*). Inner sac is continuous (*long arrow*) with spinal canal. Lipomatous component of cystic tumor is seen separated from subcutaneous fat over the buttocks by a thin septa (*open arrow*).

consistent with the fact that this is the last area of neural tube to close [7]. Ten to 20% of cases of spina bifida cystica are meningoceles and the rest are meningomyeloceles [8]. Meningomyelocele is a group of conditions in which the subcutaneous hernial sac is lined with intact meninges and contains the herniated parts of the spinal cord. The neural lesion is represented by a neural plate or an abortive, neural, tubelike structure in which the ventral half of the cord is relatively less affected than the dorsal half [7], probably because of failure of dorsal closure. There are two main types of meningomyeloceles [9]. In the first, there is a closed but flattened and deformed winged cord that floats on the posterior surface of subarachnoid space, which separates it from the vertebral bodies (Fig. 4A). In the second type, the spinal cord keeps a more anterior relation to the vertebral bodies, but its central canal is grossly dilated and the thinned-out posterior part of the spinal cord accompanies the meningeal hernia (Fig. 4B). This second kind is known as meningomyelocystocele.

In our patient, sonography, postmetrizamide CT of the spine, and MR imaging demonstrated the dual cystic components of the spina bifida cystica and the continuity of the caudal, inner sac with the spinal canal. The septated appearance of the caudal inner sac on real-time examination was consistent with meningomyelocele [4, 5]. MR clearly demonstrated the two fluid-filled components of the spina bifida cystica but not the nerve roots in the inner sac. The outer and cranial cystocele sac showed a higher signal intensity than the inner and more caudal meningomyelocele. Brandt-Zawadzki et al. [10] recently reported that the two major CSF compartments have unique signal intensities with MR imaging by spin-echo technique using TR = 2000 msec and TE = 28–56 msec. With this technique, MR can detect the subtle difference in protein concentration of ventricular and extraventricular CSF. In normal children and adults there is a concentration gradient of protein from a low level in ventricles of 6–15 mg/dl to an intermediate level in cisterna magna of 15–25 mg/dl to the highest level in the lumbar sac of 20–50 mg/dl. Fluid with more protein has more "bound water" and so a shorter T1 relaxation value and a higher MR signal intensity following RF excitation. In our patient, MR of the spine was done by using a spin-echo technique of 30 msec echo time. At TR = 500 msec, the signal intensities from CSF

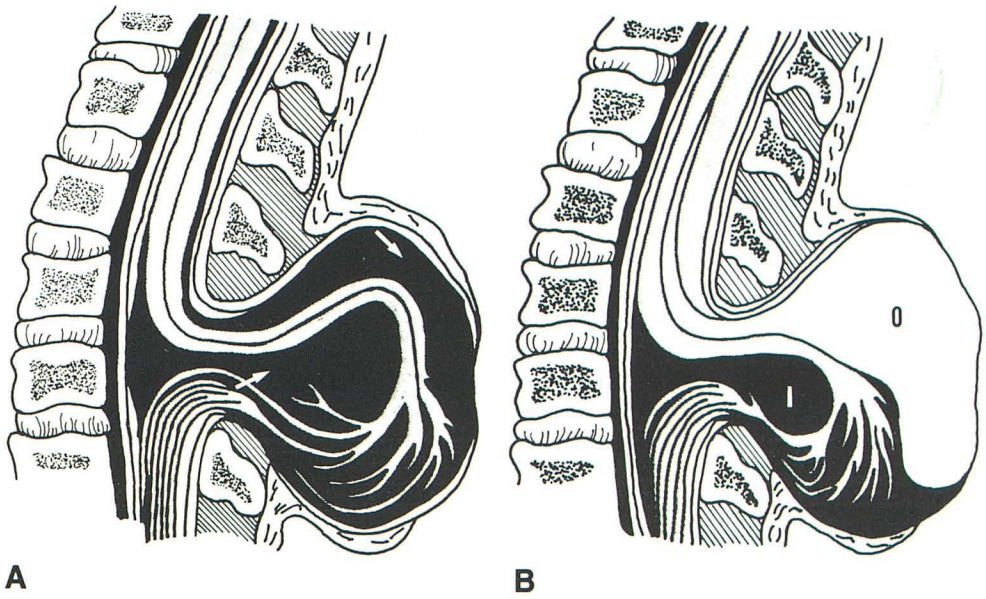

Fig. 4.—*A*, Diagram of a meningomyelocele. *Arrows* point to subarachnoid space.

***B*, Diagram of meningomyelocystocele. Spinal cord with its terminal roots is lying in meningeal sac (I), and central canal is grossly dilated and herniated to form outer and more cranial sac (O).**

are usually not strong enough to visualize subtle differences in protein content, because short TR sequences do not allow sufficient longitudinal magnetization (T1 relaxation) to occur in the fluid. Brant-Zawadzki et al. [10] studied MR characterization of intracranial CSF spaces, whereas the two fluid spaces that were compared in our patient are extracranial and peripheral along the neuroaxis. The increased protein content of the lumbar CSF is believed to be due to relatively increased permeability of the blood-CSF barrier to proteins in the spinal subarachnoid space as opposed to intracranial subarachnoid space [11]. Moreover, the CSF in the meningomyelocele sac and the cystocele sac can be presumed to have a higher protein content than that in the lumbar subarachnoid space of a normal person, secondary to the effect of the stagnation of the fluid [11]. A high signal intensity from a meningomyelocele can also be due to the presence of myelinated nerve roots within the sac, which shorten T1 time. The signal intensity difference between the contents of the two sacs in our patient was observed on MR even with spin-echo technique using TR = 500 msec. This could have been caused by excessively high protein levels within the two fluids. As the signal intensity from cystocele was higher than that from the meningomyelocele, there was probably more protein content in the former than in the latter.

If on sonographic examination of spina bifida cystica two fluid-filled sacs (one anechoic and the other septated) are seen, the possibility of it being a meningomyelocystocele should be considered. In the diagnostic evaluation of this case of lipomeningomyelocystocele, sonography could clearly demonstrate the nerve roots within the meningomyelocele, which the other two techniques could not. Evaluation of the rest of the spine (not done in our patient) and coexisting hydrocephalus or kidney anomalies is possible by sonography and is important in a child with spina bifida cystica to determine the extent of surgery required [4]. MR has the ability to characterize CSF spaces intracranially [10, 12]. In our patient, the two extracranial fluid sacs showed unique signal-intensity characteristics. It is to be hoped that this aspect of MR may improve the diagnostic evaluation of spina bifida cystica in the future. MR and CT clearly identified the lipomatous component of the herniated sac. Postmetrizamide CT of the spine is an invasive procedure when compared with sonography or MR. None of the diagnostic imaging methods we used helped to definitely prove the presence of a cystocele. It is postulated that injection of metrizamide directly into the outer anechoic sac may give a definitive diagnosis of cystocele by demonstrating the communication of the central canal with the herniated anechoic sac.

REFERENCES

1. James CCM, Lassman LP. Spinal dysraphism. An orthopedic syndrome in children accompanying occult forms. *Arch Dis Child* **1960**;35:315–327
2. Gryspeerdt GL. Myelographic assessment of occult forms of spinal dysraphism. *Acta Radiol [Diagn]* (Stockh) **1963**;1:702–717
3. James HE, Oliff M. Computed tomography in spinal dysraphism. *J Comput Assist Tomogr* **1977**;1:391–397
4. Miller JH, Reid BS, Kemberling CR. Utilization of ultrasound in the evaluation of spinal dysraphism in children. *Radiology* **1982**;143:737–740
5. Jacobs NM, Grant EG, Dagi TF, Richardson JD. Ultrasound identification of neural elements in myelomeningocele. *JCV* **1984**;12:51–53
6. Nadich TP, McLone DG, Shkolnik A, Fernback SK. Sonographic evaluation of caudal spine anomalies in children. *AJNR* **1983**;4:661–664
7. Volpe JJ. *Neurology of the newborn. Overview, dorsal induction and ventral induction.* Philadelphia: Saunders, **1981**:3–11
8. Friede RL. *Developmental neuropathology. Spina bifida and related spinal lesions.* New York: Springer-Verlag, **1975**:244–248
9. Corsellis BW Jr, ed. Malformation of the spinal cord. In: *Greenfield's neuropathology*, 3rd ed. Chicago: Year Book Medical, **1976**:369–370
10. Brant-Zawadzki M, Kelly W, Kjos B, et al. Magnetic resonance imaging and characterization of normal and abnormal intracranial cerebrospinal fluid (CSF) spaces. *Neuroradiology* **1985**;27:3–8
11. Fishman RA. Composition of cerebrospinal fluid. In: Fishman RA, ed. *Cerebrospinal fluid in diseases of the nervous system.* Philadelphia: Saunders, **1980**:168–252
12. Kjos BO, Brant-Zawadzki M, Kucharczyk W, Kelly WM, Norman D, Newton TH. Cystic intracranial lesions: magnetic resonance imaging. *Radiology* **1985**;155:363–369